ECOSYSTEMS

High Arctic Vegetation Change Mediated by Hydrological Conditions

T. Kiyo F. Campbell,[1]* Trevor C. Lantz,[1] Robert H. Fraser,[2] and Danica Hogan[3]

[1]School of Environmental Studies, University of Victoria, PO Box 1700 STN CSC, Victoria, British Columbia V8W 2Y2, Canada; [2]Centre for Mapping and Earth Observation Canada, Natural Resources Canada, 560 Rochester Street, Ottawa, Ontario K1S 5K2, Canada; [3]Environment and Climate Change Canada, Canadian Wildlife Service, Nova Plaza. 5019 – 52nd Street, PO Box 2310, Yellowknife, Northern Territory X1A 2P7, Canada

ABSTRACT

Increasing air temperatures are driving widespread changes to Arctic vegetation. In the high Arctic, these changes are patchy and the causes of heterogeneity are not well understood. In this study, we explore the determinants of high Arctic vegetation change over the last three decades on Banks Island, Northwest Territories. We used Landsat imagery (1984–2014) to map long-term trends in vegetation productivity and regional spatial data to investigate the relationships between trends in productivity and terrain position. Field sampling investigated vegetation community composition in different habitat types. Our analysis shows that vegetation productivity changes are substantial on Banks Island, where productivity has increased across about 80% of the study area. Ris-ing productivity levels can be attributed to increasing biomass of the plant communities in both upland and lowland habitats. Our analysis also shows that the magnitude of greening is mediated by terrain characteristics related to soil moisture. Shifts in tundra vegetation will impact wildlife habitat quality, surface energy balance, permafrost dynamics, and the carbon cycle; additional research is needed to explore the effects of more productive vegetation communities on these processes in the high Arctic.

Key words: Climate change; Landsat; Remote sensing; Primary production; Tundra ecosystems; Protected areas.

HIGHLIGHTS

- Vegetation productivity is increasing across the Banks Island, NT, high Arctic ecosystem.

- Greening trends are more common in upland habitats than in lowland habitats.
- The magnitude of greening is strongly influenced by moisture conditions.

Author Contributions TKFC and TCL took part in conceptualization and design; TKFC, TCL, and RHF performed research; TKFC analyzed data; TKFC, TCL, RHF, and DH contributed to methods; and TKFC, TCL, RHF, and DH wrote the manuscript.

*Corresponding author; e-mail: t.kiyo.campbell@gmail.com

INTRODUCTION

Rapidly warming temperatures are driving widespread changes to vegetation in many Arctic regions (Kaplan and New 2006; Lantz and others 2010; Myers-Smith and others 2011; Fraser and others 2014a; Ju and Masek 2016). Plot-based studies in the high Arctic show that vegetation productivity is increasing (Hudson and Henry 2009;

Hill and Henry 2011), but remote sensing studies indicate that changes are regionally variable, with extensive greening (increases in satellite-derived vegetation productivity), browning (decreases in satellite-derived vegetation productivity), and stability (no change in vegetation productivity) evident across the high Arctic (Guay and others 2014; Ju and Masek 2016; Edwards and Treitz 2017). Heterogeneity in productivity trends is likely related to continental differences in temperature (Raynolds and others 2008; Reichle and others 2018), but landscape-scale differences in biophysical variables (for example, soil moisture, surface water, vegetation type, snow conditions, and herbivory) may be contributing to the variation in vegetation responses to warming (Kotanen and Jefferies 1997; Myers-Smith and others 2015; Cameron and Lantz 2016; Martin and others 2017; Bjorkman and others 2019; Sim and others 2019). Satellite-derived trends can also be influenced by the interaction between the biophysical variation of a landscape and the spectral, spatial, and temporal resolution of the data being used (Campbell and others 2018; Myers-Smith and others 2020). Understanding the factors controlling high Arctic vegetation change is important because shifts in vegetation will impact wildlife habitat quality, surface energy balance, permafrost dynamics, and the carbon cycle (Harding and others 2002; Chapin and others 2005; Gornall and others 2007; Fraser and others 2014a; Fisher and others 2016).

In high Arctic ecosystems, topographic position is a primary determinant of soil moisture and plant community composition and productivity (Barrett and Teeri 1973; Bliss 1977; Woo and Young 1997, 2006; Ecosystem Classification Group 2013; Becker and others 2016). Upland terrain (for example, steep slopes, hilltops, and plateaus) has low soil moisture, vegetation cover, and organic soil development relative to poorly drained lowland terrain (for example, flats, alluvial terraces, or areas adjacent to water bodies) (Bliss 1977; Hines and others 2010; Ecosystem Classification Group 2013). Upland plant communities are often sparsely vegetated by prostrate dwarf shrubs and sedges, whereas lowland communities are dominated by hydrophilic sedges, grasses, and mosses (Cody 2000; CAVM Team 2003). These large differences in soil and vegetation conditions suggest that topographic position is likely to influence the nature of climate-driven vegetation change in the high Arctic.

Recent studies on Banks Island, Northwest Territories, show that upland and lowland terrain types have exhibited different hydrological responses to climate change (Fraser and others 2018; Campbell and others 2018). Over the last few decades, lowland areas across Banks Island have experienced a decline in surface water through the drying of shallow tundra ponds (Campbell and others 2018), whereas upland areas have shown an increase in surface water driven by the development of new ice-wedge melt ponds (Fraser and others 2018). A paleoecological study of high Arctic wetlands during a period of mid-twentieth-century warming also showed changes in moisture and vegetation conditions that depended on wetland type (Sim and others 2019). Given the magnitude of the recent hydrological changes on Banks Island, shifting moisture conditions could be creating diverging vegetation productivity trends among terrain types.

In this study, we combined the analysis of moderate resolution (30 m) Landsat satellite imagery (1984–2014) and regional spatial data with field sampling of vegetation communities to examine the regional scale determinants of high Arctic vegetation change over the last three decades. We hypothesized that: (1) changes in vegetation productivity would differ by habitat characteristics and topographic conditions and (2) changes in moisture would be positively associated with trends in vegetation productivity.

STUDY AREA

Banks Island is the westernmost island in the Canadian Arctic Archipelago and part of the Inuvialuit Settlement Region in the Northwest Territories. The community of Sachs Harbour is the only permanent settlement on the island, with a population of approximately 100 residents. Located within the northern or high Arctic ecozone, this area has a harsh climate with a mean annual temperature of − 12.8 °C at Sachs Harbour. Summers are short, with average daily temperatures rising above freezing for only 3 months of the year, peaking at 6.6 °C in July. Average annual precipitation is 151.5 mm, with 38% falling as rain between June and September (Environment and Climate Change Canada 2019). Mean annual temperature has increased by 3.5 °C since 1956, while summer precipitation and maximum snow water equivalent before spring melt have changed minimally (Fraser and others 2018; Mudryk and others 2018).

This study focuses on Banks Island Migratory Bird Sanctuary No. 1 (BIMBS1), which covers 20,517 km² of the southwestern side of the island (Figure 1) and is the second-largest federally pro-
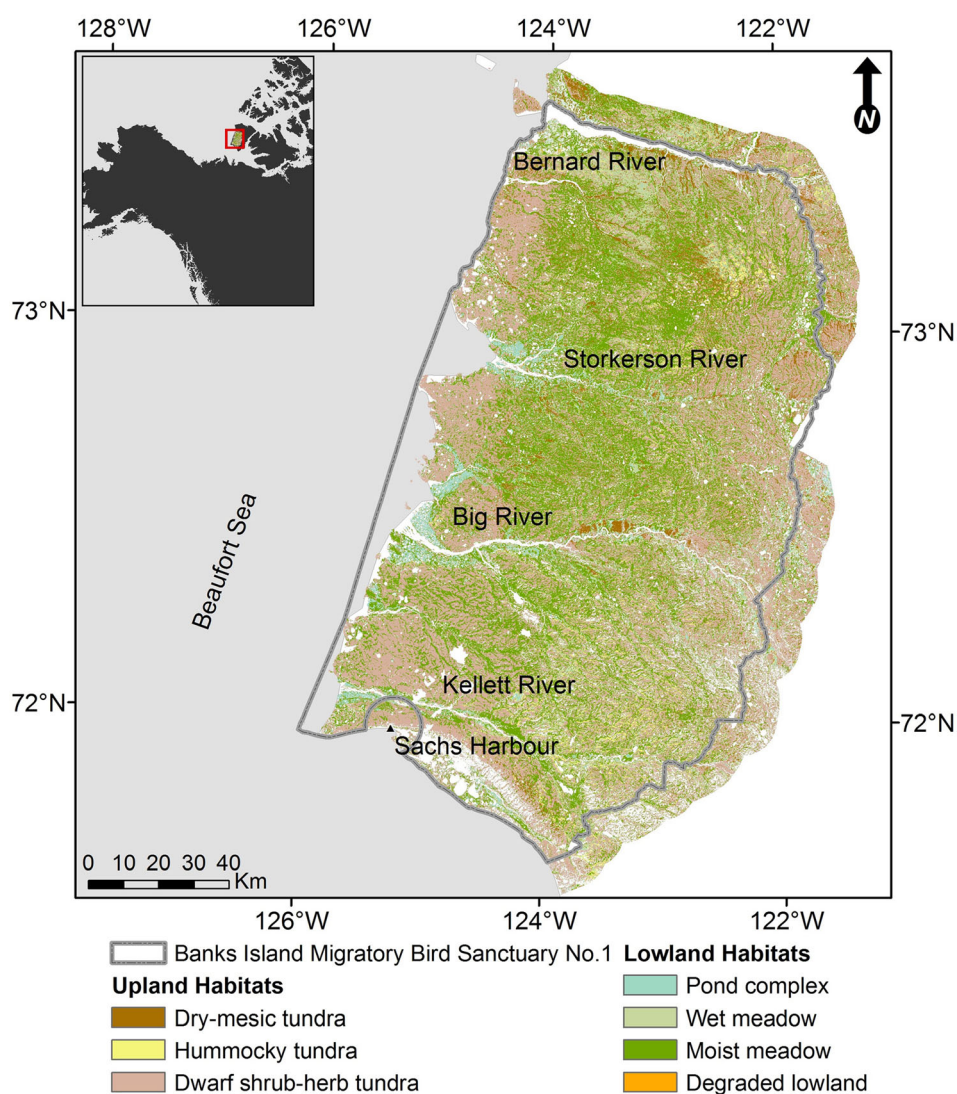
Figure 1. Map of Banks Island Migratory Bird Sanctuary No. 1, showing habitat types from the land cover classification by Hines and others (2010). Inset map at the upper left corner shows the study area on Banks Island outlined with a red box (Color figure online).

tected migratory bird sanctuary in Canada (Hines and others 2010; Ecosystem Classification Group 2013). BIMBS1 is characterized by gently rolling uplands intersected by numerous west flowing rivers with wide floodplains. Alluvial terraces in river valleys are dotted with thousands of shallow ponds and have nearly continuous vegetation cover dominated by sedges, grasses, and mosses (Hines and others 2010; Ecosystem Classification Group 2013). Upland areas are occupied by sparse to continuous dwarf shrub and herb tundra (Ecosystem Classification Group 2013). The island is underlain by continuous permafrost (French 2016), and ice-wedge polygons, non-sorted circles and stripes, and turf hummocks are widespread (Ecosystem Classification Group 2013).

BIMBS1 was created in 1961 to protect migratory birds and their habitat on Banks Island. BIMBS1 provides important nesting habitat for many migratory birds, including lesser snow geese (*Chen caerulescens caerulescens*), black brant (*Branta bernicla nigricans*), and king eiders (*Somateria spectabilis*). The main nesting colony for over 95% of the western Arctic lesser snow goose population is located at the confluence of the Egg and Big Rivers, within the migratory bird sanctuary (Hines and others 2010; Ecosystem Classification Group 2013). This colony has almost tripled in population since 1976 (Hines and others 2010; Kerbes and others 2014).

METHODS

Landsat Trends

To explore changes in vegetation productivity between 1984 and 2014, we analyzed a time series of near-annual Tasseled Cap (TC) transformed Landsat images. This time series was composed of 154 30-m-resolution images captured by the Landsat 5 TM and Landsat 7 ETM + sensors between 1984 and 2014 (Table S1). To reduce the influence of changing phenology, image acquisition dates were restricted to between July 10 and August 15 of each year. Due to cloud cover and data availability, 1 to 10 images were available each year. These images were balanced over the time series to optimize data coverage while avoiding systematic changes in the number of images over time (Figure S1 and Table S1). Images were calibrated to top-of-atmospheric reflectance using USGS coefficients (Chander and others 2009), and clouds, cloud shadows, and scan lines were masked out.

The Tasseled Cap Greenness (TCG) and Wetness (TCW) indices were calculated for each Landsat image using Landsat bands 1–5 and 7 and established coefficients (Crist and Cicone 1984; Huang and others 2002). Tasseled Cap Greenness (TCG) uses the difference between near-infrared and visible bands, making it suitable for measuring green vegetation. TCG is strongly correlated with Normalized Difference Vegetation Index (NDVI) and has shown similar results in Arctic and sub-Arctic terrain types (Fraser and others 2011; Raynolds and Walker 2016). In this study, TCG was used as opposed to NDVI, because of NDVI's greater reliance on near-infrared wavelengths, which may impact performance in areas of changing surface water and soil moisture conditions (Goswami and others 2011; Lin and others 2011; Elmendorf and others 2012; Raynolds and Walker 2016). The use of additional Landsat bands in the TCG index can reduce noise caused by varying soil and moisture conditions (Crist and Cicone 1984; Huete and others 1994). Tasseled Cap Wetness (TCW) contrasts shortwave infrared with visible and near-infrared bands which makes it sensitive to water surfaces, soil moisture, and plant moisture (Kauth and Thomas 1976; Crist and Cicone 1984). TCW has been used successfully to map changes in surface water on western Banks Island (Campbell and others 2018).

To determine per-pixel trends and test their statistical significance, Theil–Sen regression and the rank-based Mann–Kendall test were used (Hollander and Wolfe 1973; Best and Roberts 1975; Fraser and others 2014b; Olthof and others 2015; Bronaugh and Werner 2019). Cumulative Julian Day, starting from the first Landsat image in the time series, was used as the explanatory variable in these analyses. Theil–Sen regression is a nonparametric alternative to ordinary least-squares regression that uses the median of all possible pairwise slopes, instead of the mean. The rank-based Mann–Kendall test of significance is calculated by comparison with all possible pairwise slopes (Kendall and Stewart 1967).

Landscape Analysis

Our use of moderate resolution (30 m) satellite data in this study allowed for better exploration of the ecological processes mediating observed changes. Specifically, we divided the bird sanctuary into seven habitat types, which we classified as either upland or lowland habitats. This was done using a 30-m-resolution land-cover classification developed by Hines and others (2010). The classification was derived from Landsat 5 TM images acquired on July 6, 1990, and August 12, 1995, included 11 habitat types in total, and had an overall accuracy of 88%. The dry–mesic tundra, hummocky tundra, and dwarf shrub–herb tundra habitat types were grouped and classified as upland habitats (Figure 2). The lowland pond complex, wet meadow, moist meadow, and degraded lowland habitat types were grouped and classified as lowland habitats (Figure 2). The water-based, unvegetated, and unknown land-cover types from the Hines and others (2010) land-cover classification were not considered in this analysis. We calculated the area within each of the seven habitat types exhibiting significant greening, stable, and browning trends and used a Chi-square test to determine whether the frequency of pixel trends deviated from values expected based on the area covered by each habitat type. We calculated the expected number of greening, browning, and nonsignificantly trended pixels in each habitat type by multiplying the number of pixels in each trend category with the number of pixels in the habitat type and dividing by the sample size. The Chi-square test used a random subset of 300,000 pixels from upland habitats and 300,000 from lowland habitats.

To examine the biophysical factors associated with vegetative greening and browning in upland and lowland habitats, we created separate random forest regression models for upland and lowland habitat classifications, using the significant TCG trend slope as the response variable. Models were constructed using a random subset of 300,000
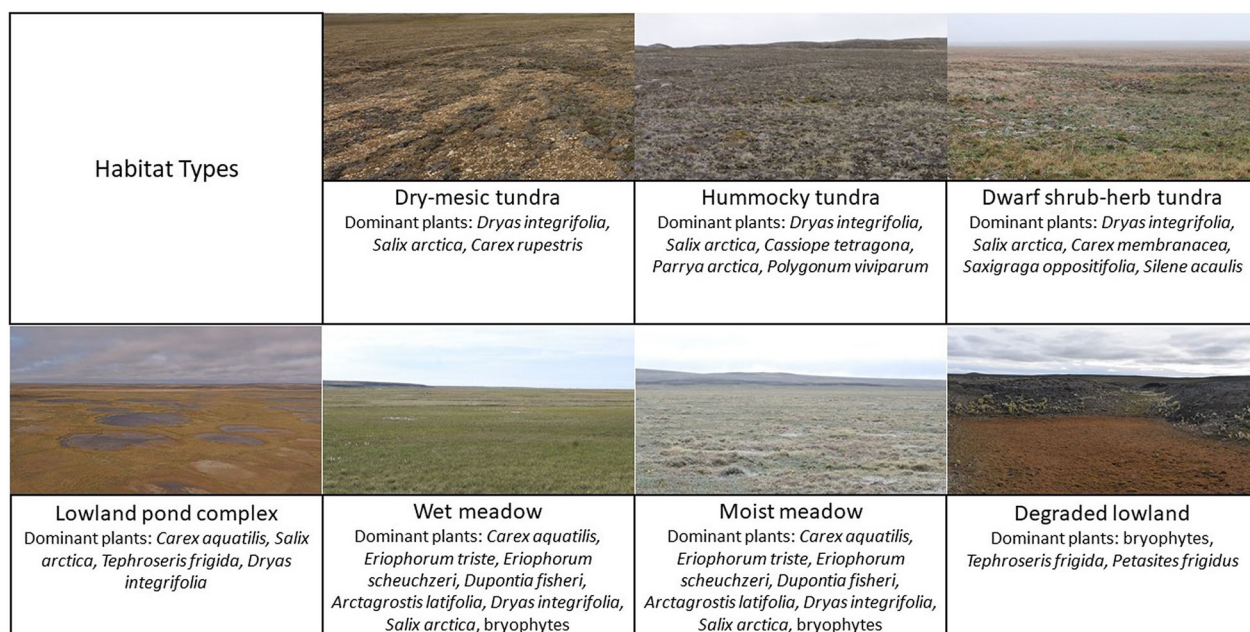
Figure 2. Example photographs from BIMBS1 of the habitat types considered in this study, as well as the dominant vascular plants found in each. Habitat types taken from the Hines and others (2010) land-cover classification of BIMBS1. Upland habitat types are shown in the upper row, whereas lowland habitat types are shown in the bottom row of the figure (Color figure online).

pixels for each habitat classification and the 'randomForest' package (Liaw and Wiener 2002), in R software version 3.3.2 (R Core Team 2016). Explanatory variables included: significant TCW trend slope, latitude, elevation, topographic slope, flow accumulation, distance from the coast, and habitat type (from Hines and others 2010). Elevation data were taken from the 5-m-resolution ArcticDEM, referenced to the WGS84 ellipsoid (Porter and others 2018). Topographic slope was calculated using the ArcticDEM and the slope tool from the ArcMap (10.4.1) surface toolset. Flow accumulation was calculated using the ArcticDEM and the fill, flow direction, and flow accumulation tools from the ArcMap (10.4.1) hydrology toolset (Jenson and Domingue 1988). The flow accumulation variable was $\log(x + 1)$-transformed to ensure normality. Distance from the coast was calculated using the Euclidean distance from a polyline, manually delineated along the western and southern coasts of BIMBS1. Spatial data that did not match the 30 m Landsat spatial resolution were aggregated using the mean value within a 30 m by 30 m area.

The variable importance function from the 'randomForest' package (Liaw and Wiener 2002) was used to determine which explanatory variables explained the most variance in TCG trends for both upland and lowland models (Liaw and Wiener 2002). Variable importance was calculated as the percentage decrease in accuracy when each explanatory variable was removed from the model; the difference in accuracy was calculated as the mean difference between the prediction errors of the out-of-bag data and the prediction errors after permuting each explanatory variable, normalized by the standard deviation of the differences (Liaw and Wiener 2002). We also used partial dependence plots to explore how the relationship between TCG trend and explanatory variables differed between upland and lowland habitat types. Partial dependence plots show the average predicted value of the response variable, at different levels of a given explanatory variable, with the influence of the other explanatory variables averaged (Friedman 2001).

Habitat Vegetation Communities

To characterize plant communities in the study area, detailed plant cover data were collected in the field over two summers (July 2017 and July–August 2018). In 2017, data were collected at 16 locations within BIMBS1. Survey sites in 2017 consisted of a single 100 m transect, oriented in a

Table 1. Observed and Expected Numbers of Greening, Browning, and Nonsignificantly Trended Pixels by Habitat Type, Based on the Chi-square Analysis of a Sample of 600,000 Pixels

	Browning		Stable		Greening	
	Observed	Expected	Observed	Expected	Observed	Expected
Lowland pond complex	**423***	90.7	**11,301***	5267.5	13,726*	20,091.8
Wet meadow	**509***	190.1	**18,582***	11,039.5	34,247*	42,108.4
Moist meadow	765	780.0	**57,336***	45,305.6	160,795*	172,810.4
Degraded lowland	**193***	8.3	**1278***	479.4	845*	1828.4
Dry–mesic tundra	17*	112.2	3223*	6514.5	**28,235***	24,848.4
Hummocky tundra	14*	56.2	1339*	3262.5	**14,410***	12,444.3
Dwarf shrub–herb tundra	217*	900.7	31,125*	52,315.0	**221,420***	199,546.3
Column totals	2138	2138	124,184	124,184	473,678	473,678

Bold numbers indicate that the observed number of pixels exceeds the expected number. Numbers with an asterisk indicate a significant difference from the expected value, using a Bonferroni correction ($p < 0.0012$) (Color figure online)

north–south direction. The percent cover of dwarf shrubs, forbs, graminoids, bryophytes, and lichens was visually estimated within 50 cm^2 quadrats at 10-m intervals along each transect. In 2018, data were collected at 40 locations within BIMBS1. Survey sites in 2018 consisted of four 50 m transects intersecting at 0 m and oriented toward the cardinal directions. The cover of dwarf shrubs, forbs, graminoids, bryophytes, and lichens were visually estimated to species within 50 cm^2 quadrats at the 25 m mark of each transect (Abraham 2014). To minimize the influence of observer error in percent cover estimations, data were binned within cover ranges (0–0.9, 1–5, 6–25, 26–50, 51–75, 76–100). To ensure that the data from both years were compatible, species were grouped into functional groups (vascular species found in Table S2–S4).

To characterize and compare the community composition among habitat types, we used a nonmetric multidimensional scaling (NMDS) analysis. This analysis used a log($x + 1$) matrix of the percent cover of each functional group. The NMDS analysis was conducted using the 'Vegan' package (Oksanen and others 2017) in R version 3.3.2 (R Core Team 2016). An analysis of similarities (ANOSIM) test was used to evaluate the dissimilarity of community composition among upland and lowland habitat types. The 'envfit' function in 'Vegan' was used to explore associations between TC trends and community composition (Oksanen and others 2017). Plots that fell within water bodies or desiccated pond basins were excluded from this analysis, as they were either entirely water or represented land cover with a different origin and substrate.

TCG Trend Contributions from Landsat Bands

To better understand the nature of vegetation change occurring on Banks Island, the contributions of each Landsat spectral band to the TCG trends were investigated using two random forest regression models (Liaw and Wiener 2002; R Core Team 2016). As previously, one model was created for upland habitats and one for lowland habitats, using a random subset of 300,000 pixels from the respective upland–lowland classification. Explanatory variables included the trend slopes for Landsat bands 1–5 and 7. Per-pixel trends over the time series (1984–2014) were calculated using Theil–Sen regression (Fraser and others 2014b; Olthof and others 2015). All significant and nonsignificant trends were considered in this analysis. The variable importance function was used to determine the wavelengths that contributed most to changes in TCG (Liaw and Wiener 2002). If no major influences from the bands existed, then importance values would resemble the TC conversion coefficients (Huang and others 2002). Partial dependence plots were used to visualize the relationships between TCG and band trends, and to investigate whether these relationships differed in upland and lowland habitats (Friedman 2001).

Landsat TM and ETM + bands 1, 3, and 4 are known to be useful wavelengths for detecting vegetation conditions (Crist and Cicone 1984; Huete and others 1994; May and others 2018). Band 1 detects visible blue wavelengths and correlates well with the other visible wavelengths in measuring green vegetation (Crist and Cicone 1984). However, band 1 is particularly useful in

reducing noise caused by varying soil and atmospheric conditions (Huete and others 1994); high band 1 importance could indicate that apparent vegetation change is an artifact of changes in soil and atmospheric conditions. Band 3 measures visible red wavelengths. Plant materials reflect more visible red light if they have lower chlorophyll content or if they are dry or desiccated (Crist and Cicone 1984; May and others 2018). High band 3 importance could indicate that vegetation change is related to an increase in vegetation with lower chlorophyll content (i.e., a change in vegetation type), or substantial changes in moisture availability. Band 4 detects near-infrared (NIR) wavelengths, which strongly correlate with plant biomass (Crist and Cicone 1984). Bands 5 and 7 detect short-wave infrared (SWIR) radiation, which is known to be sensitive to the presence of surface water (Olthof and others 2015). High importance of

bands 5 or 7 could indicate vegetation change is an artifact of a transition to or from water cover.

RESULTS

Landsat Trends and Landscape Analysis

Roughly 80% of the study area (15,628.08 km^2) exhibited a significant positive TCG trend from 1984 to 2014. Areas that showed no significant TCG trend were also common, accounting for 20% (3943.39 km^2) of the study area. Stable areas were especially prevalent in lowland habitats. Browning pixels were uncommon, making up only 0.3% (67.58 km^2) of the study area. Browning pixels were located primarily in lowland habitat areas (87% of browning pixels; Table 1) like the Bernard River valley at the northern border of BIMBS1 and at the Egg River nesting colony in the Big River valley (Figure 3B). The extent of greening also
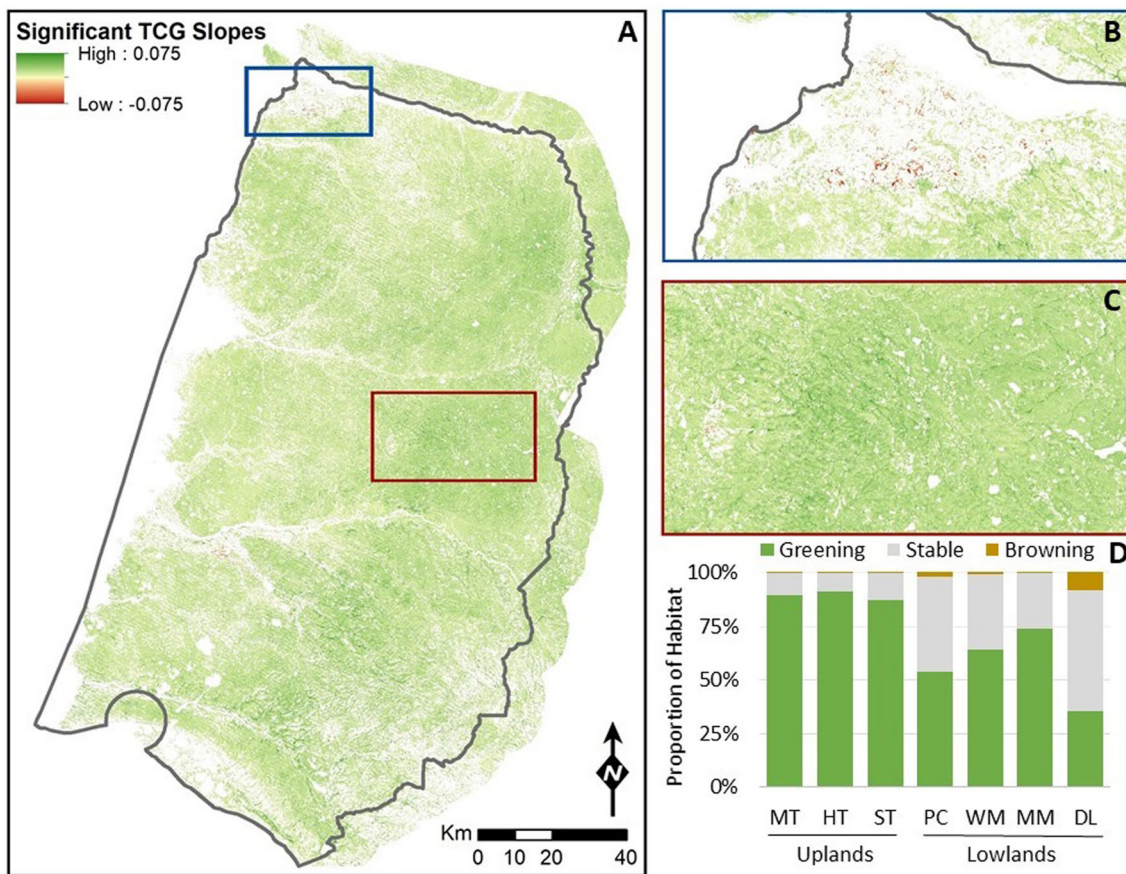

Figure 3. (A) Significant TCG trend slopes ($p < 0.05$) across the study area of BIMBS1. (B) Enlarged inset showing an alluvial terrace adjacent to the Bernard River. (C) Enlarged inset showing an upland area northeast of the Egg River Snow Goose nesting colony. (D) The proportion of pixels with significant positive (greening) or negative (browning) TCG trend slopes ($p < 0.05$) in each habitat type; pixels were classified as stable (gray) if there was no significant trend. Habitat types include: dry–mesic tundra (MT), hummocky tundra (HT), dwarf shrub–herb tundra (ST), lowland pond complex (PC), wet meadow (WM), moist meadow (MM), and degraded lowland (DL) (Color figure online).

differed in upland and lowland habitats. The proportion of significantly greening pixels in the three upland habitats ranged from 87 to 92%, whereas the proportion of significantly greening pixels in the lowland habitats ranged from 35 to 74% (Figure 3). A Chi-square test confirmed that the amount of greening, browning, and stability was associated with the upland and lowland classifications ($p < 0.001$) (Table 1). All lowland habitat types, except moist meadow, had more browning and stable pixels, and fewer greening pixels than would be expected based on the proportion of the study area covered by each habitat type. Moist meadow had the expected amount of browning pixels, but more stable pixels than expected and fewer greening pixels than expected. All upland habitat types had more greening, and fewer browning and stable pixels than expected (Table 1).

The random forest models parameterized to predict changes in TCG explained a similar proportion of the total variance in upland ($R^2 = 0.418$) and lowland ($R^2 = 0.385$) habitats, but the importance of explanatory variables differed between models. The most important variables in the upland model were (1) flow accumulation, (2) habitat type, (3) topographic slope, and (4) TCW slope, which all increased model accuracy by over 100% (Figure 4). The most important variables in the lowland model were (1) TCW slope, (2) topographic slope, (3) habitat type, (4) latitude, (5) distance from the coast, and (6) flow accumulation, which all increased model accuracy by over 100% (Figure 4). TCW slope was particularly important in the lowland model, increasing model accuracy

by 94% more than the next most important variable.

The partial dependence plot for habitat type shows that upland habitat types had consistently higher predicted TCG trends, relative to lowland habitat types. Hummocky tundra had the highest predicted TCG trend, and the degraded lowland and pond complex habitat types had the lowest predicted TCG trends (Figure 5A). The partial dependence plots for TCW trend show that higher greening was associated with pixels where surface water and soil moisture were also increasing (Figure 5B). This effect was intensified in lowland areas where TCG showed larger increases and decreases in response to changes in TCW.

Topographic slope had opposite effects on TCG trends in upland versus lowland habitats. In upland habitats, TCG trends were highest in flatter areas, while in lowland habitats, flat areas had the lowest TCG trends (Figure 5C). In both upland and lowland habitats, increases in TCG were higher at high levels of flow accumulation (Figure 5D). The partial dependence plots for latitude show that increases in TCG were highest at mid-latitudes for upland habits and low-to-mid-latitudes for lowland habitats (Figure 5E). The partial dependence plots for distance from the coast show that inland areas had higher average greening (Figure 5F).

Habitat Vegetation Communities

The NMDS ordination plotted in Figure 6 shows considerable heterogeneity among habitat types, but a clear distinction between upland and lowland habitats. A pairwise comparison of the upland and lowland sites produced an R_{ANOSIM} statistic of 0.442
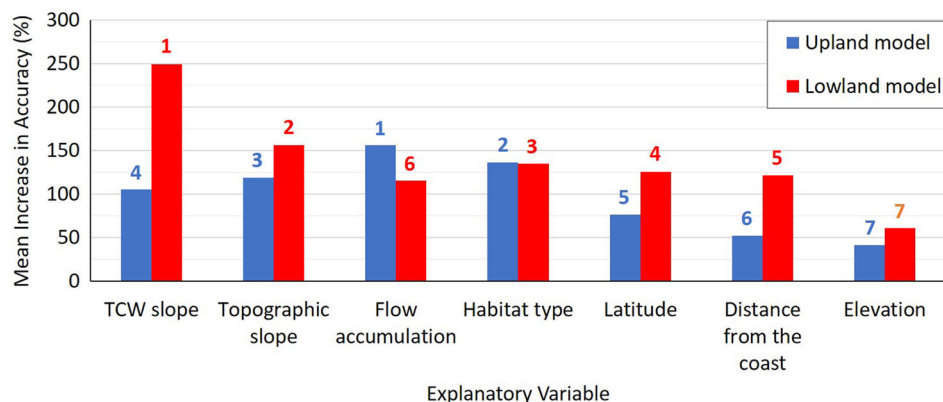

Figure 4. Variable importance for the upland and lowland random forest models explaining vegetation change with moisture and terrain related variables. Variable importance is measured as the percentage increase in accuracy when individual explanatory variables are included in the model; calculated using the mean difference between the prediction errors of the out-of-bag data and the prediction errors after permuting each explanatory variable, normalized by the standard error of the differences (Liaw and Wiener 2002) (Color figure online).
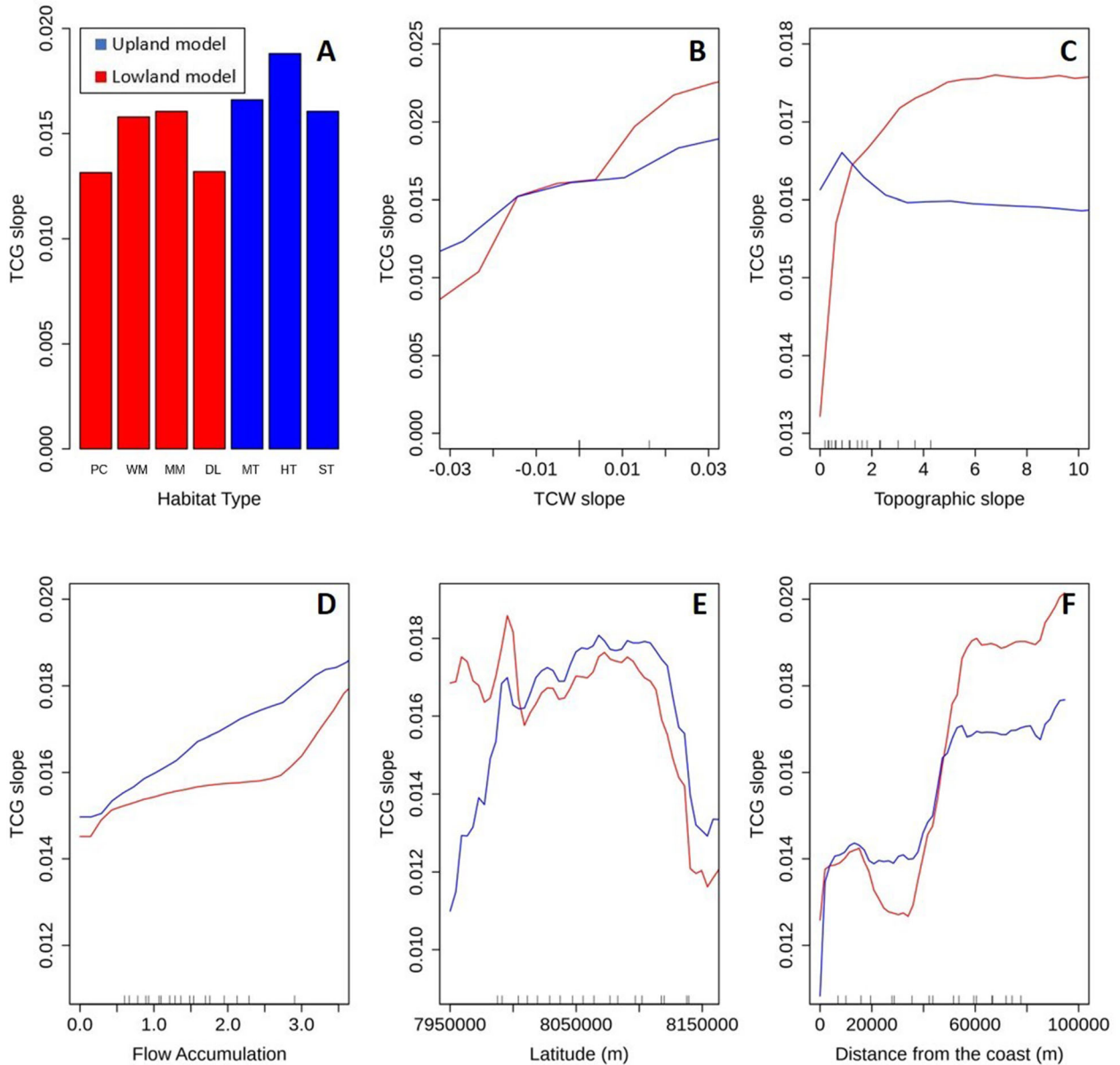
Figure 5. Partial dependence plots showing the most important explanatory variables from both upland and lowland random forest regressions. Class variables are shown as bar graphs, while continuous variables are shown as line graphs. Red bars and lines represent the lowland model, and blue bars and lines represent the upland model: (**A**) habitat type, (**B**) TCW trend slope, (**C**) topographic slope, (**D**) flow accumulation, (**E**) latitude, and (**F**) distance from the coast. The y-axis shows the mean predicted TCG trend slope, at different levels of the given explanatory variable, with the influence of the other explanatory variables averaged (Friedman 2001). Habitat types include: dry–mesic tundra (MT), hummocky tundra (HT), dwarf shrub–herb tundra (ST), lowland pond complex (PC), wet meadow (WM), moist meadow (MM), and degraded lowland (DL) (Color figure online).

($p < 0.001$), indicating moderate separation between upland and lowland community composition. Upland communities were associated with high forb and lichen cover, and lowland communities were associated with the dominance of bryophytes. Dwarf shrubs and graminoids were common in both uplands and lowlands, as indicated by the vectors shown in Figure 6, which are oriented perpendicular to the separation between upland and lowland habitats. The ordination of community composition also shows that upland quadrats associated with increasing TCG had high forb cover and highly variable cover of dwarf shrub and graminoids, whereas lowland quadrats associ-
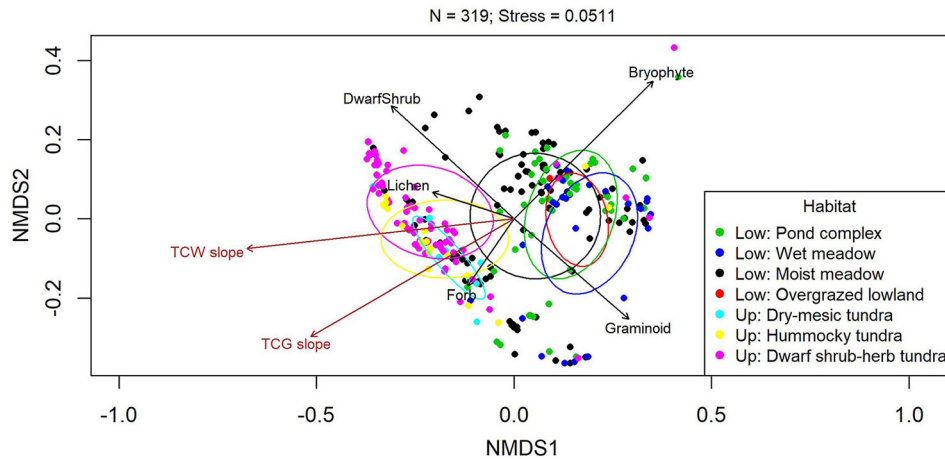
Figure 6. NMDS ordination (stress = 0.0511) plot showing similarity and dissimilarity of vegetation community composition among habitat types. Each point (n = 319) on the ordination represents an individual field quadrat, and its proximity to other points represents the similarity in plant community composition, with close meaning more similar. Ellipses represent the standard deviation of NMDS1 and NMDS2 for each habitat type. The black arrows show the direction and magnitude of significant associations between functional group cover and the NMDS scores for each quadrat. The brown arrows show the direction and magnitude of significant associations between the TC trend slopes and the NMDS scores for each quadrat (Color figure online).

ated with increasing TCG had high forb and graminoid cover. Lower TCG slopes were associated with bryophyte dominated lowland habitats.

TCG Trend Contributions from Landsat Bands

Random forest models parameterized to determine the contributions of each Landsat band to the TCG trends both explained a large proportion of the total

Figure 7. Variable importance for the upland and lowland random forest models explaining TCG pixel trends with Landsat band trends. Importance is measured as the percentage increase in accuracy when each explanatory variable is included in the model; calculated using the mean difference between the prediction errors of the out-of-bag data and the prediction errors after permuting each explanatory variable, normalized by the standard deviation of the differences (Liaw and Wiener 2002) (Color figure online).

variance in upland (R^2 = 0.878) and lowland (R^2 = 0.911) habitat types. In both models, Landsat band 4 was over five times more important than any other band (Figure 7). The order of importance did not match TC conversion coefficient values (Huang and others 2002). The partial dependence plot (Figure 8D) shows a positive association between the trend slopes of TCG and band 4, suggesting that the increase in TCG is being driven by increases in plant biomass.
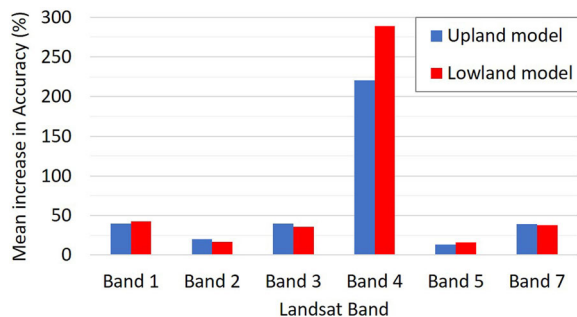
DISCUSSION

The widespread nature of the greening on western Banks Island suggests that this change is the product of rapid increases in air temperature observed across the western Arctic (Hansen and others 2010; Vincent and others 2015). Since 1950, mean summer (June–August) temperatures have increased by 1–2 °C and mean spring (March–May) and fall (September–November) temperatures have increased by 2–4 °C (Hansen and others 2010; NASA GISS 2014). These changes are larger than the difference in average temperature between some northern and southern Arctic ecoregions in the Northwest Territories (Ecosystem Classification Group 2012; Ecosystem Classification Group 2013). Ground-based studies using experimental warming, repeat survey, and space-for-time approaches all suggest that tundra vegetation change is linked to increasing air and ground temperatures, which can extend the length of the growing season and
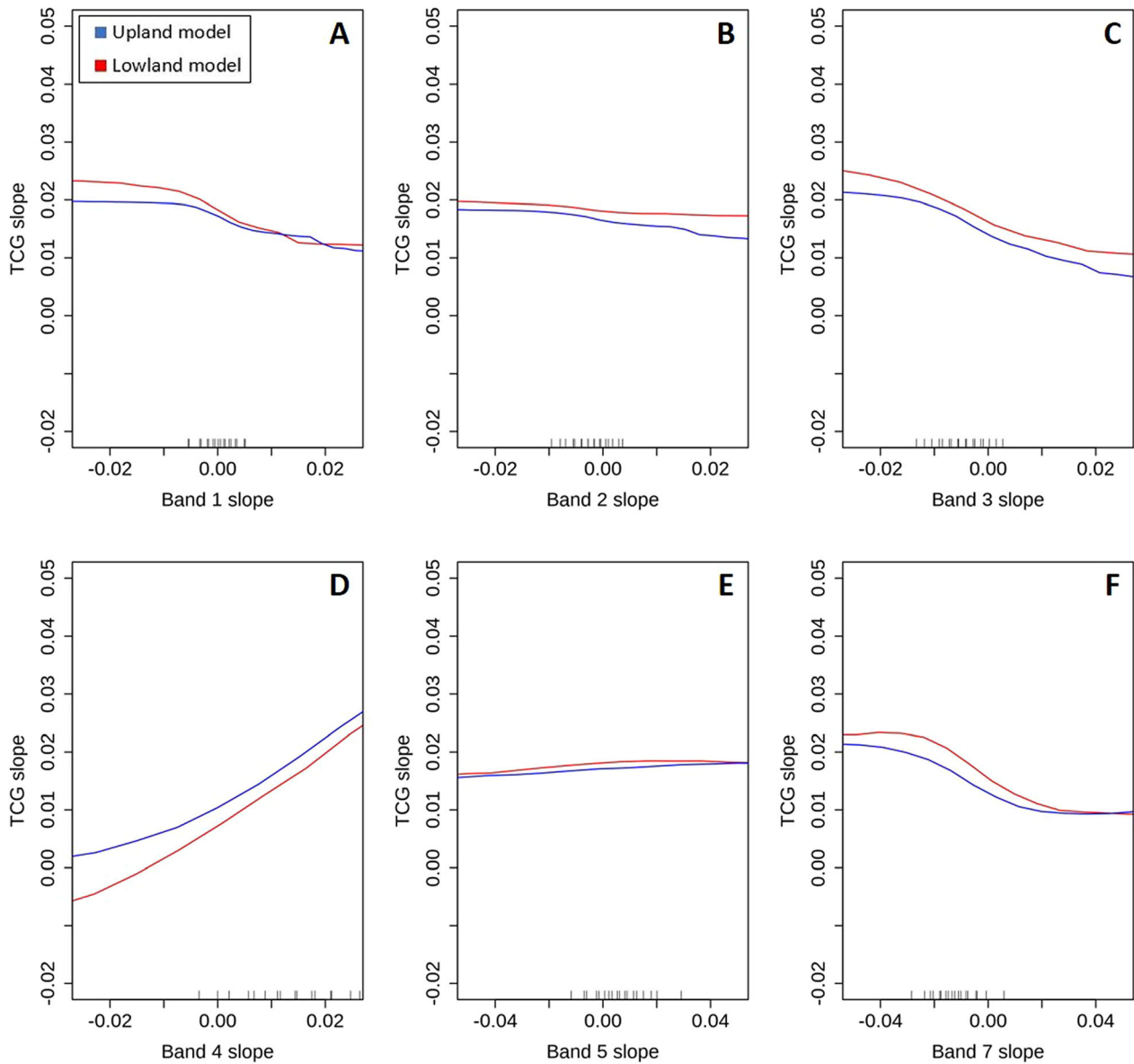
Figure 8. Partial dependence plots for each Landsat band trend slope, from both upland and lowland random forest regression models. Red lines represent the lowland model and blue lines represent the upland model: (**A**) band 1, (**B**) band 2, (**C**) band 3, (**D**) band 4, (**E**) band 5, and (**F**) band 7. The y-axis shows the mean predicted TCG trend slope, at different levels of the given explanatory variable, with the influence of the other explanatory variables averaged (Friedman 2001) (Color figure online).

increase the level of plant available nutrients (Chapin and others 1995; Walker and others 2006; Elmendorf and others 2015).

The correspondence between hydrological indicator variables and the magnitude of greening suggests that climate-driven vegetation change is being mediated by moisture availability across the study area. Variables related to moisture potential, such as flow accumulation, slope, and TCW trends, were among the most important predictors of variation in productivity trends within BIMBS1. In

upland habitats, flow accumulation, which is a proxy for the discharge of overland and subsurface flow, was the most important factor in explaining changes in productivity. The observation that higher greening occurred in areas with high flow accumulation levels indicates that tundra vegetation receiving moisture and nutrients from upslope areas can more effectively capitalize on increased summer temperatures compared to drier areas (Billings and Mooney 1968; Webber 1978; Guo and others 2012; Atkinson and Treitz 2013; Johansson

and others 2013; Becker and others 2016; Niittynen and Luoto 2017). This is consistent with research by Naito and Cairns (2011) and Tape and others (2012), showing that shrub expansion on the North Slope of Alaska was greatest in drainage areas with large potential for moisture accumulation. Flow pathways are likely to be particularly important on Banks Island where the spring freshet is the largest annual influx of water and one of the only times of the year that surface runoff occurs (Lewkowicz and French 1982). The association between greening and topographic slope in the upland habitats also shows that greening was highest in flatter areas where surface water can accumulate (Riedlinger and Berkes 2001; Fraser and others 2018). In lowland habitat types, the TCW trend, which describes long-term changes in moisture, was the most important factor in explaining productivity changes. Our observation that greening was highest in lowland areas with increasing moisture trends is also consistent with numerous studies, indicating that soil moisture can strongly influence northern vegetation change (Elmendorf and others 2012; Myers-Smith and others 2015; Cameron and Lantz 2016).

Our observation that greening was less widespread in lowland habitats also suggests that soil moisture mediates the response of tundra vegetation to warming. Water bodies and wetlands are more common in lowland habitats (Ecosystem Classification Group 2013), where higher moisture availability has facilitated the long-term development of productive plant communities dominated by hydrophilic sedges, grasses, and mosses (Cody 2000; CAVM Team 2003; Woo and Young 2006). It is likely that plant communities in these habitats are less responsive to warming because productivity is already relatively high in lowland areas (Hines and others 2010; Ecosystem Classification Group 2013) and there is less potential for vegetation expansion and greening. This is consistent with our observation that greening in lowland habitats was highest on slopes, which are likely to have intermediate moisture levels and lower vegetation cover.

Discrete areas of vegetation browning in lowland habitats indicate that long-term changes in moisture may be contributing to reductions in aboveground biomass and productivity in some areas. Lowland areas with significant reductions in TCW experienced the lowest average greening levels. Recent research also shows that lowland pond complexes and degraded lowlands, which had the highest proportions of browning pixels, have experienced a large loss of surface water (Campbell

and others 2018). Overgrazing from lesser snow geese, which can reduce aboveground biomass and is known to be occurring in some areas of BIMBS1, may also be contributing to the areas of decreasing productivity (Jefferies and others 1979; Kotanen and Jefferies 1997; Hines and others 2010).

Our analysis suggests that trends in TCG are linked to the growth of existing vegetation, rather than shifts in the abundance of some functional groups (Figures 6, 7, and 8). Variation in community composition at upland sites was not correlated with the trend in TCG, indicating that greening is not associated with increases in the dominance of a single functional group as has been described in the low Arctic (Tremblay and others 2012; Fraser and others 2014a; Frost and Epstein 2014; Moffat and others 2016). This explanation is also consistent with warming experiments in high Arctic tundra, which show increases in biomass from existing vegetation, and little evidence of species replacements (Hudson and Henry 2009; Hill and Henry 2011). Taken together, this suggests that the greening we observed in upland habitats is likely the result of increases in forb and dwarf shrub biomass. Greening in lowland habitats has probably been driven by the growth of forbs and graminoids. Browning in lowland habitats is likely related to decreases in forbs and graminoids exposing bare peat or a bryophyte carpet (Hines and others 2010). Although still vegetated, an exposed bryophyte carpet is also more susceptible to desiccation, leading to reduced productivity and discoloration (Proctor 2000; Proctor and Tuba 2002; May and others 2018). Future research should investigate whether species dominance is shifting toward more moisture-tolerant species within functional groups.

Changes in the productivity of tundra ecosystems are significant because they are likely to impact surface energy balance, permafrost and active layer dynamics, and wildlife habitat quality (Harding and others 2002; Chapin and others 2005; Gornall and others 2007; Fraser and others 2014a; Fisher and others 2016). Increasing vegetation biomass may affect surface energy balance, as denser vegetation can decrease summer and winter albedo, contributing to further warming trends (Chapin and others 2005; Loranty and others 2011). Changes in vegetation can also alter permafrost conditions and terrain stability (Gornall and others 2007; Kokelj and Jorgenson 2013; Fisher and others 2016). Additional research on the nature of high Arctic greening is vital because vegetation canopy density and moss layer characteristics have a substantial influence on active layer thickness and the quantity of carbon stored in permafrost (Gornall and

others 2007; Fisher and others 2016). A range of species (lesser snow geese, black brant, king eider, Peary caribou, and muskox) rely on BIMBS1, particularly lowland habitats, for forage and protection during nesting and calving periods (Slattery and Alisauskas 2007; Sachs Harbour and Joint Secretariat 2008). Understanding the nature of vegetative change, especially shifts in the abundance of forage plants, is also critical to evaluate the impacts of climate change on wildlife within this protected area and to enable effective management of the Migratory Bird Sanctuary. Effective conservation and management of the wildlife resources within the sanctuary are particularly important to the Inuvialuit of Sachs Harbour, who rely on many of the species within BIMBS1 for cultural and subsistence purposes (Sachs Harbour and Joint Secretariat 2008).

CONCLUSION

Tundra vegetation on Banks Island, Northwest Territories, has undergone significant changes over the last three decades. Vegetation productivity has increased across about 80% of BIMBS1, which can be attributed to increases in biomass of the dominant vegetation in upland and lowland habitats. The widespread nature of these changes suggests that they are linked to recent increases in air temperature, but a strong association between the magnitude of greening and flow accumulation, long-term changes in moisture, and slope also suggests that observed greening is being mediated by hydrological conditions. Greening trends were particularly prevalent in upland habitat types, where the largest increases were found along drainage pathways with relatively flat slopes, hummocky tundra, and areas with long-term increases in moisture. Substantial areas of lowland habitats did not experience significant changes in productivity; however, greening was still the dominant trend in these areas. Greening in lowland habitats was highest in areas with long-term increases in moisture, and in meadow habitat types and sloped terrain. Understanding high Arctic vegetation change is important because it will impact wildlife habitat and ecological feedbacks to the climate system. Future studies should investigate the effects of more productive vegetation on permafrost conditions and wildlife habitat selection.

ACKNOWLEDGEMENTS

REFERENCES

Abraham KF. 2014. Goose foraging in arctic habitats with a protocol for a rapid ground based assessment of its impacts on northern plant communities. Canadian Wildlife Service Internal Report, Winnipeg, MB, Canada.

Atkinson DM, Treitz P. 2013. Modeling biophysical variables across an Arctic latitudinal gradient using high spatial resolution remote sensing data. Arct Antarct Alp Res 45:161–78.

Barrett PE, Teeri JA. 1973. Vascular plants of the Truelove Inlet region, Devon Island. Arctic 23:58–67.

Becker MS, Davies TJ, Pollard WH. 2016. Ground ice melt in the high Arctic leads to greater ecological heterogeneity. J Ecol 104:114–24.

Best DJ, Roberts DE. 1975. Algorithm AS 89: the upper tail probabilities of Spearman's ρ. Applied Statistics 24:377–9.

Billings WD, Mooney HA. 1968. The ecology of Arctic and alpine plants. Biol Rev Camb Philos 43:481–529.

Bjorkman AD, Criado MG, Myers-Smith IH, Ravolainen V, Jonsdottir IS, Westergaard KB, Lawler JP, Aronsson M, Bennett B, Gardfjell H, Heiomarsson S, Stewart L, Normand S. 2019. Status and trends in Arctic vegetation: evidence from experimental warming and long-term monitoring. Ambio 0044–7447:1–15.

Bliss LC. 1977. Truelove Lowland, Devon Island, Canada: A high Arctic ecosystem. Edmonton, Alberta, Canada: The University of Alberta Press.

Bronaugh D, Werner A. 2019. Zyp: Zhang + Yue-Pilon trends package. R package version 0.10-1.1. https://CRAN.R-project.org/package=zyp.

Cameron EA, Lantz TC. 2016. Drivers of tall shrub proliferation adjacent to the Dempster Highway, Northwest Territories Canada. Environ Res Lett 11:045006.

Campbell TKF, Lantz TC, Fraser RH. 2018. Impacts of climate change and intensive lesser snow goose (Chen caerulescens caerulescens) activity on surface water in high Arctic pond complexes. Remote Sens 10:1892.

CAVM Team. 2003. Circumpolar Arctic vegetation map. Conservation of Arctic Flora and Fauna (CAFF) Map No. 1, U.S. Fish and Wildlife Service, Anchorage Alaska.

Chander G, Markham BL, Helder DL. 2009. Summary of current radiometric calibration coefficients for Landsat MSS, TM,

ETM + , and EO-1 ALI sensors. Remote Sens Environ 113:893–903.

Chapin FSIII, Shaver GR, Giblin AE, Nadelhoffer KJ, Laundre JA. 1995. Response of Arctic tundra to experimental and observed changes in climate. Ecology 76:694–711.

Chapin FSIII, Sturm M, Serreze MC, McFadden JP, Key JR, Lloyd AH, McGuire AD, Rupp TS, Lynch AH, Schimel JP, Beringer J, Chapman WL, Epstein HE, Euskirchen ES, Hinzman LD, Jia G, Ping C-L, Tape KD, Thompson CDC, Walker DA, Welker JM. 2005. Role of land-surface changes in Arctic summer warming. Science 310:657–60.

Cody WJ. 2000. Flora of the Yukon Territory. 2nd edn. Ottawa, Canada: NRC Research Press.

Crist EP, Cicone RC. 1984. A physically-based transformation of thematic mapper data: the TM tasseled cap. IEEE T Geosci Remote 22:256–63.

Ecosystem Classification Group. 2012. Ecological regions of the Northwest Territories—Southern Arctic. Department of Environment and Natural Resources, Government of the Northwest Territories, Yellowknife, NT, Canada: 1–170.

Ecosystem Classification Group. 2013. Ecological regions of the Northwest Territories—Northern Arctic. Department of Environment and Natural Resources, Government of the Northwest Territories, Yellowknife, NT, Canada: 1–157.

Edwards R, Treitz P. 2017. Vegetation greening trends at two sites in the Canadian Arctic: 1984–2015. Arctic, Antarctic, and Alpine Research 49:601–19.

Elmendorf SC, Henry GHR, Hollister RD, Björk RG, Boulanger-Lapointe N, Cooper EJ, Cornelissen JHC, Day TA, Dorrepaal E, Elumeeva TG, Gill M, Gould WA, Harte J, Hik DS, Horgaard A, Johnson DR, Johnstone JF, Jónsdóttir IS, Jorgenson JC, Klanderud K, Klein JA, Koh S, Kudo G, Lara M, Lévesque E, Magnússon B, May JL, Mercado-Daz JA, Michelsen A, Molau U, Myers-Smith IH, Oberbauer SF, Onipchenko VG, Rixen C, Schmidt NM, Shaver GR, Spasojevic MJ, Þórhallsdóttir ÞE, Tolvanen A, Troxler T, Tweedie CE, Villareal S, Wahren C-H, Walker X, Webber PJ, Welker JM, Wipf S. 2012. Plot-scale evidence of tundra vegetation change and links to recent summer warming. Nat Clim Change 2:453–7.

Elmendorf SC, Henry GHR, Hollister RD, Fosaa AM, Gould WA, Hermanutz L, Hofgaard A, Jónsdóttir IS, Jorgenson JC, Lévesque E, Magnusson B, Molau U, Myers-Smith IH, Oberbauer SF, Rixen C, Tweedie CE, Walker MD. 2015. Experiment, monitoring, and gradient methods used to infer climate change effects on plant communities yield consistent patterns. Proc Nat Acad Sci USA 112:448–52.

Environment and Climate Change Canada. 2019. Climate data online. Available from http://climate.weather.gc.ca/climate_normals/ [6 August 2019].

Fisher JP, Estop-Aragones C, Thierry A, Charman DJ, Wolfe SA, Hartley IP, Murton JB, Williams M, Phoenix GK. 2016. The influence of vegetation and soil characteristics on active-layer thickness of permafrost soils in boreal forest. Glob Change Biol 22:3127–40.

Fraser RH, Olthof I, Carriere M, Deschamps A, Pouliot D. 2011. Detecting long-term changes to vegetation in northern Canada using the Landsat satellite image archive. Environmental Research Letters 6:045502.

Fraser RH, Lantz TC, Olthof I, Kokelj SV, Sims RA. 2014a. Warming-induced shrub expansion and lichen decline in the western Canadian Arctic. Ecosystems 17:1151–68.

Fraser RH, Olthof I, Kokelj SV, Lantz TC, Lacelle D, Brooker A, Wolfe S, Schwarz S. 2014b. Detecting landscape changes in high latitude environments using Landsat trend analysis: 1 Visualization. Remote Sens 6:11533–57.

Fraser RH, Kokelj SV, Lantz TC, McFarlane-Winchester M, Olthof I, Lacelle D. 2018. Climate sensitivity of high Arctic permafrost terrain demonstrated by widespread ice-wedge thermokarst on Banks Island. Remote Sens 10:954.

French HM. 2016. The tundra and polar semi-desert landscapes of Banks Island and Prince Patrick Island, western Canadian Arctic. Cuadern Investig Geografica 42:321–40.

Friedman J. 2001. Greedy function approximation: the gradient boosting machine. Ann Stat 29:1189–232.

Frost GV, Epstein HE. 2014. Tall shrub and tree expansion in Siberian tundra ecotones since the 1960s. Glob Change Biol 20:1264–77.

Gornall JL, Jonsdottir IS, Woodin SJ, Van der Wal R. 2007. Arctic mosses govern below-ground environment and ecosystem processes. Oecologia 153:931–41.

Goswami S, Gamon JA, Tweedie CE. 2011. Surface hydrology of an Arctic ecosystem: Multiscale analysis of a flooding and draining experiment using spectral reflectance. J Geophys Res 116:G00I07.

Guay KC, Beck PA, Berner LT, Goetz SJ, Baccini A, Buermann W. 2014. Vegetation productivity patterns at high northern latitudes: a multi-sensor satellite data assessment. Glob Change Biol 20:3147–58.

Guo L, Cai Y, Belzile C, MacDonald RW. 2012. Sources and export fluxes of inorganic and organic carbon and nutrient species from the seasonally ice-covered Yukon River. Biogeochemistry 107:187–206.

Hansen J, Ruedy R, Sato M, Lo K. 2010. Global surface temperature change. Rev Geophys 48:RG4004.

Harding R, Kuhry P, Christensen TR, Sykes MT, Dankers R, van der Linden S. 2002. Climate feedbacks at the tundra-taiga interface. Ambio 47–55.

Hill GB, Henry GHR. 2011. Responses of high Arctic wet sedge tundra to climate warming since 1980. Glob Change Biol 17:276–87.

Hines JE, Latour PB, Squires-Taylor C, Moore S. 2010. The effects on lowland habitat in the Banks Island Bird Sanctuary Number 1, Northwest Territories, by the growing colony of lesser snow geese (Chen caerulescens caerulescens). Environment Canada Occasional Paper 118:8–26.

Hollander M, Wolfe DA. 1973. Nonparametric statistical methods. New York: John Wiley & Sons. pp 185–94.

Huang C, Wylie B, Yang L, Homer C, Zylstra G. 2002. Derivation of a tasseled cap transformation based on Landsat 7 at-satellite reflectance. Int J Remote Sens 23:1741–8.

Hudson JMG, Henry GHR. 2009. Increased plant biomass in a high Arctic heath community from 1981 to 2008. Ecology 90:2657–63.

Huete A, Justice C, Liu H. 1994. Development of vegetation and soil indices for MODIS-EOS. Remote Sens Environ 49:224–34.

Jefferies RL, Jensen A, Abraham KF. 1979. Vegetational development and the effect of geese on vegetation at La Perouse Bay, Manitoba. Can J Bot 57:1439–50.

Jenson SK, Domingue JO. 1988. Extracting topographic structure from digital elevation data for geographic information system analysis. Photogramm Eng Rem S 54:1593–600.

Johansson M, Callaghan TV, Bosio J, Akerman HJ, Jackowicz-Korczynski M, Christensen TR. 2013. Rapid responses of permafrost and vegetation to experimentally increased snow cover in sub-Arctic Sweden. Environ Res Lett 8:035025.

Ju J, Masek JG. 2016. The vegetation greenness trend in Canada and US Alaska from 1984–2012 Landsat data. Remote Sens Environ 176:1–16.

Kaplan JO, New M. 2006. Arctic climate change with a 2 °C global warming: Timing, climate patterns and vegetation change. Climate Change 79:213–41.

Kauth RJ, Thomas GS. 1976. The tasseled cap—a graphic description of the spectral-temporal development of agricultural crops as seen by Landsat. LARS Symposia 159:41–51.

Kendall MG, Stuart AS. 1967. Advanced theory of statistics. London, UK: Charles Griffin and Company. p 2.

Kerbes RH, Meeres KM, Alisauskas RT. 2014. Surveys of nesting lesser snow geese and Ross's geese in Arctic Canada, 2002–2009. *Arctic Goose Joint Venture Special Publication, U.S. Fish and Wildlife Service, Washington, D.C. and Canadian Wildlife Service, Ottawa, Ontario* 987-0-9881233-1-1.

Kokelj SV, Jorgenson MT. 2013. Advances in thermokarst research. Permafr Periglac Process 24:108–19.

Kotanen PM, Jefferies RL. 1997. Long-term destruction of subarctic wetland vegetation by lesser snow geese. Ecoscience 4:179–82.

Lantz TC, Gergel SE, Kokelj SV. 2010. Spatial heterogeneity in the shrub tundra ecotone in the Mackenzie Delta region, Northwest Territories: Implications for Arctic environmental change. Ecosystems 13:194–204.

Lewkowicz AG, French HM. 1982. The hydrology of small runoff plots in an area of continuous permafrost, Banks Island, N.W.T.. *Hydrology in Permafrost Regions—Proc. 4th Can. Permafrost Conf.* 151–162.

Liaw A, Wiener M. 2002. Classification and regression by randomForest. R News 2:18–22.

Lin DH, Johnson DR, Andresen C, Tweedie CE. 2011. High spatial resolution decade-time scale land cover change at multiple locations in the Beringian Arctic (1948–2000s). Environ Res Lett 7:025502.

Loranty MM, Goetz SJ, Beck PSA. 2011. Tundra vegetation effects on pan-Arctic albedo. Environ Res Lett 6:024014.

Martin AC, Jeffers ES, Petrokofsky G, Myers-Smith I, Macias-Fauria M. 2017. Shrub growth and expansion in the Arctic tundra: An assessment of controlling factors using an evidence-based approach. Environ Res Lett 12:085007.

May JL, Parker T, Unger S, Oberbauer SF. 2018. Short term changes in moisture content drive strong changes in Normalized Difference Vegetation Index and gross primary productivity in four Arctic moss communities. Remote Sens Environ 212:114–20.

Moffat ND, Lantz TC, Fraser RH, Olthof I. 2016. Recent vegetation change (1980–2013) in the tundra ecosystems of the Tuktoyaktuk Coastlands, NWT, Canada. Arct Antarct Alp Res 48:581–97.

Mudryk LR, Derksen C, Howell S, Laliberte F, Thackeray C, Sospedra-Alfonso R, Vionnet V, Kushner PJ, Brown R. 2018. Canadian snow and sea ice: historical trends and projections. Cryosphere 12:1157–76.

Myers-Smith IH, Hik DS, Kennedy C, Cooley D, Johnstone JF, Kenney AJ, Krebs CJ. 2011. Expansion of canopy-forming willows over the twentieth century on Herschel Island, Yukon Territory, Canada. Ambio 40:610–23.

Myers-Smith IH, Elmendorf SC, Beck PSA, Wilmking M, Hallinger M, Blok D, Tape KD, Rayback SA, Macias-Fauria M, Forbes BC, Speed JDM, Boulanger-Lapointe N, Rixen C, Levesque E, Schmidt NM, Baittinger C, Trant AJ, Hermanutz L, Collier LS, Dawes MA, Lantz TC, Weijers S, Jorgensen RH, Buchwal A, Buras A, Naito AT, Ravolainen V, Schaepman-Strub G, Wheeler JA, Wipf S, Guay KC, Hik DS, Vellend M. 2015. Climate sensitivity of shrub growth across the tundra biome. Nat Clim Change 5:887–91.

Myers-Smith IH, Kerby JT, Phoenix GK, Bjerke JW, Epstein HE, Assmann JJ, John C, Andreu-Hayles L, Angers-Blondin S, Beck PSA, Berner LT, Bhatt US, Bjorkman AD, Blok D, Bryn A, Christiansen CT, Cornelissen JHC, Cunliffe AM, Elmendorf SC, Forbes BC, Goetz SJ, Hollister RD, de Jong R, Loranty MM, Macias-Fauria M, Maseyk K, Normand S, Olofsson J, Parker TC, Parmentier FJW, Post E, Schaepman-Strub G, Stordal F, Sullivan PF, Thomas HJD, Tommervik H, Treharne R, Tweedie CE, Walker DA, Wilmking M, Wipf S. 2020. Complexity revealed in the greening of the Arctic. Nat Clim Change 10:106–17.

NASA GISS. 2014. Surface temperature analysis: Global maps from GHCN v3 data. Available from https://data.giss.nasa.gov/gistemp/maps/ [19 December 2019].

Naito AT, Cairns DM. 2011. Relationships between Arctic shrub dynamics and topographic derived hydrologic characteristics. Environ Res Lett 6:045506.

Niittynen P, Luoto M. 2017. The importance of snow in species distribution models of Arctic vegetation. Ecography 41:1024–37.

Oksanen J, Blanchet FG, Friendly M, Kindt R, Legendre P, McGlinn D, Minchin PR, O'Hara RB, Simpson GL, Solymos P, Stevens MHH, Szoecs E, Wagner H. 2017. *Vegan: Community ecology package*. R package version 2.4-4. https://CRAN.R-project.org/package=vegan.

Olthof I, Fraser RH, Schmitt C. 2015. Landsat-based mapping of thermokarst lake dynamics on the Tuktoyaktuk coastal plain: Northwest Territories, Canada since 1985. Remote Sens Environ 168:194–204.

Porter C, Morin P, Howat I, Noh M-J, Bates B, Peterman K, Keesey S, Schlenk M, Gardiner J, Tomko K, Willis M, Kelleher C, Cloutier M, Husby E, Foga S, Nakamura H, Platson M, Wethington, M, Williamson C, Bauer G, Enos J, Arnold G, Kramer W, Becker P, Doshi A, D'Souza C, Cummens P, Laurier F, Bojesen M. 2018. ArcticDEM. Available from https://doi.org/10.7910/DVN/OHHUKH [19 December 2019]. *Harvard Dataverse V1*.

Proctor MCF. 2000. The bryophyte paradox: tolerance of desiccation, evasion of drought. Plant Ecol 151:41–9.

Proctor MCF, Tuba Z. 2002. Poikilohydry and homoihydry: Antithesis or spectrum of possibilities? New Phytol 156:327–49.

R Core Team. 2016. R: A language and environment for statistical computing. *R Foundation for Statistical Computing*, Vienna, Austria. URL https://www.R-project.org/.

Raynolds MK, Comiso JC, Walker DA, Verbyla D. 2008. Relationship between satellite-derived land surface temperatures, Arctic vegetation types, and NDVI. Remote Sens Environ 112:1884–94.

Raynolds MK, Walker DA. 2016. Increased wetness confounds Landsat-derived NDVI trends in the central Alaska North Slope region, 1985–2011. Environmental Research Letters 11:085004.

Reichle LM, Epstein HE, Bhatt US, Raynolds MK, Walker DA. 2018. Spatial heterogeneity of the temporal dynamics of Arctic tundra vegetation. Geophys Res Lett 45:9206–15.

Riedlinger D, Berkes F. 2001. Contributions of traditional knowledge to understanding climate change in the Canadian Arctic. Polar Rec 37:315–28.

Sachs Harbour, Wildlife Management Advisory Council (NWT), Joint Secretariat. 2008. Sachs Harbour Community Conservation Plan 5–109.

Sim TG, Swindles GT, Morris PJ, Galka M, Mullan D, Galloway JM. 2019. Pathways for ecological change in Canadian high Arctic wetlands under rapid twentieth century warming. Geophys Res Lett 46:4726–37.

Slattery SM, Alisauskas RT. 2007. Distribution and habitat use of Ross' and lesser snow geese during late brood rearing. J Wildlife Manage 71:2230–7.

Tape KD, Hallinger M, Welker JM, Ruess RW. 2012. Landscape heterogeneity of shrub expansion in Arctic Alaska. Ecosystems 15:711–24.

Tremblay B, Levesque E, Boudreau S. 2012. Recent expansion of erect shrubs in the low Arctic: Evidence from eastern Nunavik. Environ Res Lett 7:035501.

Vincent LA, Zhang X, Brown RD, Feng Y, Mekis E, Milewska EJ, Wan H, Wang XL. 2015. Observed trends in Canada's climate and influence of low-frequency variability modes. J Climate 28:4545–60.

Walker MD, Wahren CH, Hollister RD, Henry GHR, Ahlquist LE, Alatalo JM, Bret-Harte MS, Calef MP, Callaghan TV, Carroll AB, Epstein HE, Jónsdóttir IS, Klein JA, Magnusson B, Molau U, Oberbauer SF, Rewa SP, Robinson CH, Shaver GR, Suding KN, Thompson CC, Tolvanen A, Totland O, Turner PL, Tweedie CE, Webber PJ, Wookey PA. 2006. Plant community responses to experimental warming across the tundra biome. Proc Nat Acad Sci USA 103:1342–6.

Webber PJ. 1978. Spatial and temporal variation of the vegetation and its productivity, Barrow Alaska. Vegetation and Production Ecology of an Alaskan Arctic Tundra. edited by L.L. Tieszen. Springer-Verlag, New York 37–112.

Woo M-K, Young KL. 1997. Hydrology of a small drainage basin with polar oasis environment, Fosheim Peninsula, Ellesmere Island, Canada. Permafr Periglac Process 8:257–77.

Woo M-K, Young KL. 2006. High Arctic wetlands: their occurrence, hydrological characteristics and sustainability. J Hydrol 320:432–50.